



## Wild-type levels of ceramide and ceramide-1-phosphate in the retina of ceramide kinase-like-deficient mice

Christine Graf<sup>a</sup>, Satoru Niwa<sup>a</sup>, Matthias Müller<sup>b</sup>, Bernd Kinzel<sup>b</sup>, Frédéric Bornancin<sup>a,\*</sup>

<sup>a</sup> Novartis Institutes for BioMedical Research, Brunnerstrasse 59, A-1235 Vienna, Austria

<sup>b</sup> Novartis Institutes for BioMedical Research, Forum 1, CH-4056 Basle, Switzerland

### ARTICLE INFO

#### Article history:

Received 3 June 2008

Available online 12 June 2008

#### Keywords:

Ceramide

Ceramide-1-phosphate

Kinase

Retinitis pigmentosa

Ceramide kinase

### ABSTRACT

Ceramide kinase-like (CerkL) is the most recently identified member of the sphingolipid metabolizing enzyme family. This protein is believed to have ceramide kinase (CerK) activity; however, this has not been clarified yet. We generated CerkL-deficient (*CerkL*<sup>−/−</sup>) mice, measured ceramide (Cer) and ceramide-1-phosphate (C1P) levels in isolated retina, and compared them to levels measured in *CerkL*<sup>−/−</sup> and WT retinas. We also labeled *CerkL*<sup>−/−</sup>, *CerkL*<sup>−/−</sup>, and WT retinas with <sup>33</sup>P orthophosphate to measure and compare *de novo* phosphorylation of Cer. Whereas *CerkL*<sup>−/−</sup> retinas displayed decreased C1P and enhanced Cer, and lacked the capacity to phosphorylate Cer, *CerkL*<sup>−/−</sup> retinas were indistinguishable from WT retinas with regard to Cer and C1P levels, and in their ability to phosphorylate Cer. Altogether, our results do not support the hypothesis that CerkL is a second CerK enzyme impacting on Cer levels in the retina. CerkL, if active enzymatically, might use a novel, not yet described, lipid substrate.

© 2008 Elsevier Inc. All rights reserved.

Inherited retinal degenerative diseases feature a progressive loss of mature photoreceptor cells as a result of apoptosis. One such disorder is retinitis pigmentosa, which is genetically heterogeneous and is the main cause of adult blindness [1]. Previous linkage analysis revealed a novel autosomal recessive retinitis pigmentosa locus on human chromosome 2, leading to the identification of ceramide kinase-like (CerkL), a new member of the diacylglycerol kinase (DAGK) family named for its homology with ceramide kinase (CerK) [2].

CerK was recently identified and defines a new class, distinct from sphingosine and (di)acylglycerol kinases [3]. Ceramide (Cer) and its conversion to ceramide-1-phosphate (C1P) by CerK are emerging as important factors in the regulation of apoptosis [4–6]. It is currently hypothesized that CerkL is a specific retinal CerK [2]. Thus, deficiency in CerkL might cause an increase in Cer, leading to apoptosis and development of retinitis pigmentosa. First attempts in vitro with recombinant CerkL failed to show CerK activity in CerkL [7,8]. However, it cannot be excluded that the re-

combinant expression and assay systems used in these early studies failed to provide conditions allowing for CerkL activity. To address this further we have generated CerkL-deficient (*CerkL*<sup>−/−</sup>) mice and have profiled their Cer and C1P levels as well as their capacity to phosphorylate Cer *de novo*, in isolated retinas. This tissue was selected based on high CerkL expression and because mutation in the *CerkL* gene leads to retinitis pigmentosa [2]. Our findings demonstrate that CerkL, despite its close sequence homology to CerK, is unlikely to have Cer kinase activity.

### Material and methods

**Generation of *CerkL*<sup>−/−</sup> mice.** CerkL genomic sequences corresponding to *CerkL* intron 4, exon 5, and intron 5 were amplified from BALB/c mouse genomic DNA and subcloned into the vector pRAY 2loxP 2FRT, resulting in the plasmid CERKL target. Subcloned sequences were compared to sequences available from the mouse genome informatics (MGI) database (MGI ID: 3037816). BALB/c mouse ES cell culture was performed with primary X-ray-inactivated embryonic fibroblasts derived from DR4 mice. ES cells were transfected by electroporation using 12 µg of linearized pCerkL target. Transfected ES cells were selected for neomycin resistance using 0.2 mg/ml geneticin (Invitrogen). Ten days after transfection, 400 G418-resistant ES cell clones were isolated and analyzed by polymerase chain reaction (PCR) for homologous recombination. ES cells were extracted in 50 µl of lysis buffer (10 mM Tris-HCl

**Abbreviations:** Cer, ceramide; CerK, ceramide kinase; CerkL, ceramide kinase-like; C1P, ceramide-1-phosphate; DAGK, diacylglycerol kinase; KO, knockout; LPA, lysophosphatidic acid; PA, phosphatidic acid; PCR, polymerase chain reaction; PGP, phosphatidylglycerol phosphate; WT, wild-type.

\* Corresponding author. Present address: Novartis Institutes for BioMedical Research, Forum 1, CH-4056 Basle, Switzerland. Fax: +41 61 32 44464.

E-mail address: [frederic.bornancin@novartis.com](mailto:frederic.bornancin@novartis.com) (F. Bornancin).

(pH 8.0), 0.05% SDS, 50 µg/ml proteinase K), and diagnostic PCR was performed using 1 µl of crude ES cell extract in a total volume of 20 µl. PCRs were performed using the Qiagen Taq PCR Master Mix.

1st PCR: sense primer: Neo-4: TCC TCG TGC TTT ACG GTA; anti-sense primer: CERKL-rev1: ATG GCT TCA AAG GCA GAT. Mix: 1 µl genomic DNA, 1 µl sense primer (10 µM), 1 µl antisense primer (10 µM), 10 µl Qiagen Taq PCR Master Mix, 7 µl H<sub>2</sub>O. Cycling conditions: 95 °C for 3 min, then 35 cycles (95 °C for 30 s, 50 °C for 30 s, 72 °C for 2 min) followed by 72 °C for 3 min. One microliter of the first reaction was used for nested PCR using the same mix and cycling conditions but with 25 cycles. 2nd PCR: sense primer: Neo-5: CTA TCG CCT TCT TGA CGA; antisense primer: CERKL-rev3: AGC TTG GAA ACT TCC TGC.

To control for the presence of the loxP element 5' of *CerKL* exon 5, 1 µl of genomic DNA (10 ng/µl) was analyzed in a total volume of 20 µl using the Eppendorf MasterMix. Analysis was performed on a 4% agarose gel. PCR: sense primer: CERKL lox fw: GTC ATG TGC TAC AAT CGT; antisense primer: CERKL lox rev: CTA TGT ACA TGC TGA TGT C. Mix: 1 µl genomic DNA, 1 µl sense primer (10 µM), 1 µl antisense primer (10 µM), 8 µl Eppendorf MasterMix, 9 µl H<sub>2</sub>O. Cycling conditions: 95 °C for 3 min, then 38 cycles (95 °C for 30 s, 55 °C for 30 s, 72 °C for 15 s) followed by 72 °C for 3 min. Southern blotting was performed on 5 µg of genomic DNA, digested with 30 U of the restriction enzyme and separated on a 0.9% agarose gel. After denaturation the DNA was blotted on a Hybond N+ membrane (GE Healthcare) followed by UV crosslinking. Hybridization with the <sup>32</sup>P-labeled DNA probe (Rediprime II Random prime labeling kit, GE Healthcare) was performed in Perfect Plus Hybridization buffer (Sigma) at 65 °C overnight. After washing of the hybridized membrane, image analysis was performed using a phosphorimager. Targeted BALB/c ES cells were injected into C57Bl/6 host blastocysts, which were then transferred into pseudopregnant CB6F1 foster mothers. Chimeric offspring were identified by coat pigmentation (white (BALB/c) on a black (C57Bl/6) background). White offspring indicated the germline transmission of the targeted ES cells and were further analyzed for their correct genotype. The *CerKL* knockout (KO) mouse line was named C-CERKL<sup>tm1NPA</sup>, according to the guidelines of the International Committee on Standardized Genetic Nomenclature for Mice. In order to excise *CerKL* exon 5, C-CERKL<sup>tm1NPA</sup> mice were mated with BALB/c Cre deleter females (C-TgN(CMV-Cre)#Cgn) [9], resulting in the excision of the floxed exon 5. Offspring were analyzed for their genotype by PCR, performed on genomic DNA prepared from tail biopsies. Primers used for amplification were CERKL<sup>lox</sup>fw1 and Neo, resulting in an amplification product of 550 bp for the KO allele, and CERKL<sup>lox</sup>fw1 and CERKL<sup>lox</sup>rev, resulting in an amplification product of 133 bp for the WT allele. Cycling conditions were as follows: 34 cycles of 94 °C for 30 s, 55 °C for 30 s, and 68 °C for 1 min 30 s + 10 min at 68 °C. The established mouse line with mutated *CerKL* expression was named C-CERKL<sup>TM2Npa</sup>.

The animals were kept under standard housing conditions. Investigations were performed on 10- to 12-week-old mice. The experimental procedures met all regulations and standards as approved by the Austrian and Swiss governments.

**Determination of ceramide and C16-C1P levels by LC/ESI/MS/MS (LC/MS).** Ceramide concentrations in retinas were determined as described in [10]. Briefly, 100 µl of retinal homogenate was spiked with internal standard (C17-ceramide, Avanti Polar Lipids; final concentration 1 ng/ml), and 750 µl methanol/chloroform (2:1) was added. After mixing and incubation for 1 h at 48 °C, the mixture was cooled to room temperature and 75 µl KOH (1 M) was added, followed by incubation for 1 h at 37 °C. The pH was then adjusted to ~5 by addition of 10% acetic acid (approx. 100 µl). After addition of 750 µl chloroform the samples were mixed for 3 min

and centrifuged (2600 rpm, 10 min). The organic layer was dried *in vacuo* and reconstituted in an eluent mixture of 80% B and 20% A (see below). Samples were chromatographed on a Luna C18 column (3 µm, 2 × 50 mm; Phenomenex), which was eluted with a gradient (eluent A: 5 mM ammonium acetate in acetonitrile containing 2% methanol, 1% acetic acid, 0.25% tetrahydrofuran; eluent B: 5 mM ammonium acetate in methanol containing 1% acetic acid and 0.25% tetrahydrofuran). The gradient was shaped as follows: 4 min at 1% B isocratic, then in 6 min to 100% B at a flow-rate of 0.6 ml/min and a column temperature of 50 °C. The MRM transitions monitored (*m/z*) and the optimal collision energies in [V] were as follows [ceramide acyl chain length/Q1 MRM transition; Q3 MRM transition/optimal collision energy]: [C12/482.39;264.5/33] [C16/538.44;264.5/33] [C16-Dh/540.46;284.5/39] [C17/552.41;264.5/41] [C18/566.43;264.5/35] [C18-Dh/568.51;284.5/33] [C18:1/564.48;264.5/35] [C20/594.47;264.5/37] [C24/650.54;264.5/41] [C24-Dh/652.54;284.6/37] [C24:1/648.54;264.5/45] [C24:1-Dh/650.53;284.5/41]. For calibration, dilutions of 0.05–2500 ng/ml of the individual ceramides were added from stock solutions in methanol/chloroform (2:1). Analytical standards were all obtained from Avanti Polar Lipids.

For C16-C1P measurements, retinas were homogenized in a glass tissue grinder on ice in 100 µl cold PBS. Homogenates were transferred into a glass tube. Five-hundred microliters of methanol and 250 µl chloroform were added. Samples were spiked with an internal standard (C8-C1P, Avanti Polar Lipids). After vortexing, samples were incubated at 48 °C for 16 h. The sample was finally centrifuged for 10 min at 2600 rpm at 4 °C. The supernatant was dried in an autosampler vial. Samples were dissolved in mobile phase and subjected to high performance liquid chromatography (HPLC 1100; Agilent), performed as described by Boath et al. [11]. In short, a Supelco Discovery C18 HS column (2.1 mm × 50 mm, 3 µm particle size) was used and eluted with a gradient (eluent A: 5 mM ammonium formate + 1% formic acid in methanol/water (70/30) + 2% tetrahydrofuran; eluent B: 5 mM ammonium formate + 1% formic acid in methanol + 2% tetrahydrofuran; 70–100% B in 1.8 min) at a flow of 400 µl/min at 60 °C. Electrospray-ionization with tandem mass spectroscopy (MS/MS) using an API 4000 QTrap instrument (MDS Sciex) was employed to detect C1P with positive ionization. The optimal collision energy for C16-C1P was +51 V; the multiple reactions monitoring transition followed were *m/z* 618.6/264.1.

**Determination of C1P using radiolabeling and 2D-TLC analysis.** Immediately following their isolation, retinas were pre-incubated in 200 µl phosphate-free medium (MEM Earl) supplemented with 10% FCS (dialyzed against TBS). The medium was renewed after 1 h and incubation was continued for another hour. After removal of medium, retinas were incubated with 200 µl phosphate-free medium containing 200 µCi/ml <sup>33</sup>P orthophosphate (GE Healthcare) for 2 h. At the end of the labeling period, medium was removed by centrifugation, then retinas were washed twice in PBS, snap frozen, and stored at –80 °C. Lipid extraction and analysis using 2D-TLC was performed as described in [11].

**Preparation of lipid standards.** Standards were prepared using <sup>33</sup>P ATP by reacting purified *Escherichia coli* diacylglycerol kinase (Calbiochem), which has promiscuous activity, with either 1-palmitoyl-rac-glycerol (Sigma), to produce lysophosphatidic acid (LPA), or with 1,2-di-palmitoyl-sn-glycerol (Sigma) to produce phosphatidic acid (PA), or with dipalmitoylphosphatidylglycerol (Avanti Polar Lipids) to produce phosphatidylglycerol phosphate (PGP). The reaction protocol was identical to that used for CerK [10], except that the assay buffer contained 3 mM MgCl<sub>2</sub> instead of CaCl<sub>2</sub>. C1P was produced using C16 ceramide and purified CerK as described previously [10]. Lipid extraction was performed as described in [11].

## Results and discussion

### Generation and validation of *CerKL*<sup>-/-</sup> mice

*CerKL* KO in BALB/c embryonic stem cells was achieved by the substitution of the intron 4 to intron 5 region of *CerKL* with a construct harboring a neomycin resistance gene cassette and the *CerKL* exon 5 flanked by loxP elements. This exon encodes the C2 domain and most of the C3 domain of CerKL, which are expected to be critical determinants for activity based on homology with all other lipid kinases of the DAGK family; exon 5 bears the putative ATP-binding motif VCVGGDG [7]. Homologous recombination of the targeting plasmid into the *CerKL* locus was verified by Southern hybridization (Fig. 1A). To generate *CerKL*<sup>-/-</sup> mice, chimeric males were crossed with BALB/c Cre deleter females [9] that express the recombinase in the fertilized oocyte, resulting in deletion of the floxed fragment in all cells of the organism. *CerKL* KO in the offspring was validated by PCR (Fig. 1B).

*CerKL*<sup>-/-</sup> animals were viable and fertile and there was no obvious phenotypical difference compared with WT animals. In particular, we analyzed retinas of *CerKL*<sup>-/-</sup> animals. All retinas appeared fully formed and all layers were represented histologically (data not shown). That *CerKL*<sup>-/-</sup> retinas did not exhibit any signs of degeneration may not be surprising given the BALB/c background of the animals. In fact, these findings suggest that ablation of CerKL may have pathophysiological consequences on pigmented retinal

epithelia only, consistent with the established link between mutation in CerKL and development of retinitis pigmentosa. Furthermore, the lack of retinal pathology in BALB/c *CerKL*<sup>-/-</sup> mice enabled to perform all lipid measurements using histologically comparable retinal specimen from WT, *CerKL*<sup>-/-</sup>, and *CerKL*<sup>-/-</sup> animals.

### Measurements of Cer and C16-C1P levels in the retina of *CerKL*<sup>-/-</sup> mice

If CerKL has Cer kinase activity, Cer and C1P levels may be regulated by CerKL. Ablation of CerK, the closest protein homolog of CerKL, was recently reported to impact on C1P and Cer levels [10]. We therefore isolated retina, a tissue reported to express high levels of CerKL [2], and measured the concentration of C16-C1P, a major C1P species, in *CerKL*<sup>-/-</sup> animals in comparison to *CerKL*<sup>-/-</sup> and WT animals. C16-C1P was reduced by 80% in *CerKL*<sup>-/-</sup> retinas (Fig. 2A), confirming observations already reported for other tissues [10]. By contrast, the C16-C1P levels found in *CerKL*<sup>-/-</sup> retinas did not significantly differ from WT levels (Fig. 2A). Next we measured Cer concentrations. In *CerKL*<sup>-/-</sup> retinas, Cer levels were all significantly increased, irrespective of the length of the ceramide chain (C14, C16, C18, C18:1, C20, C24, C24:1) (Fig. 2B). By contrast, in *CerKL*<sup>-/-</sup> retinas, the levels of all Cer species were identical to those found in WT retinas (Fig. 2B). These results therefore indicate that ablation of CerKL, in contrast to ablation of CerK, does not significantly impact on Cer and C1P levels.

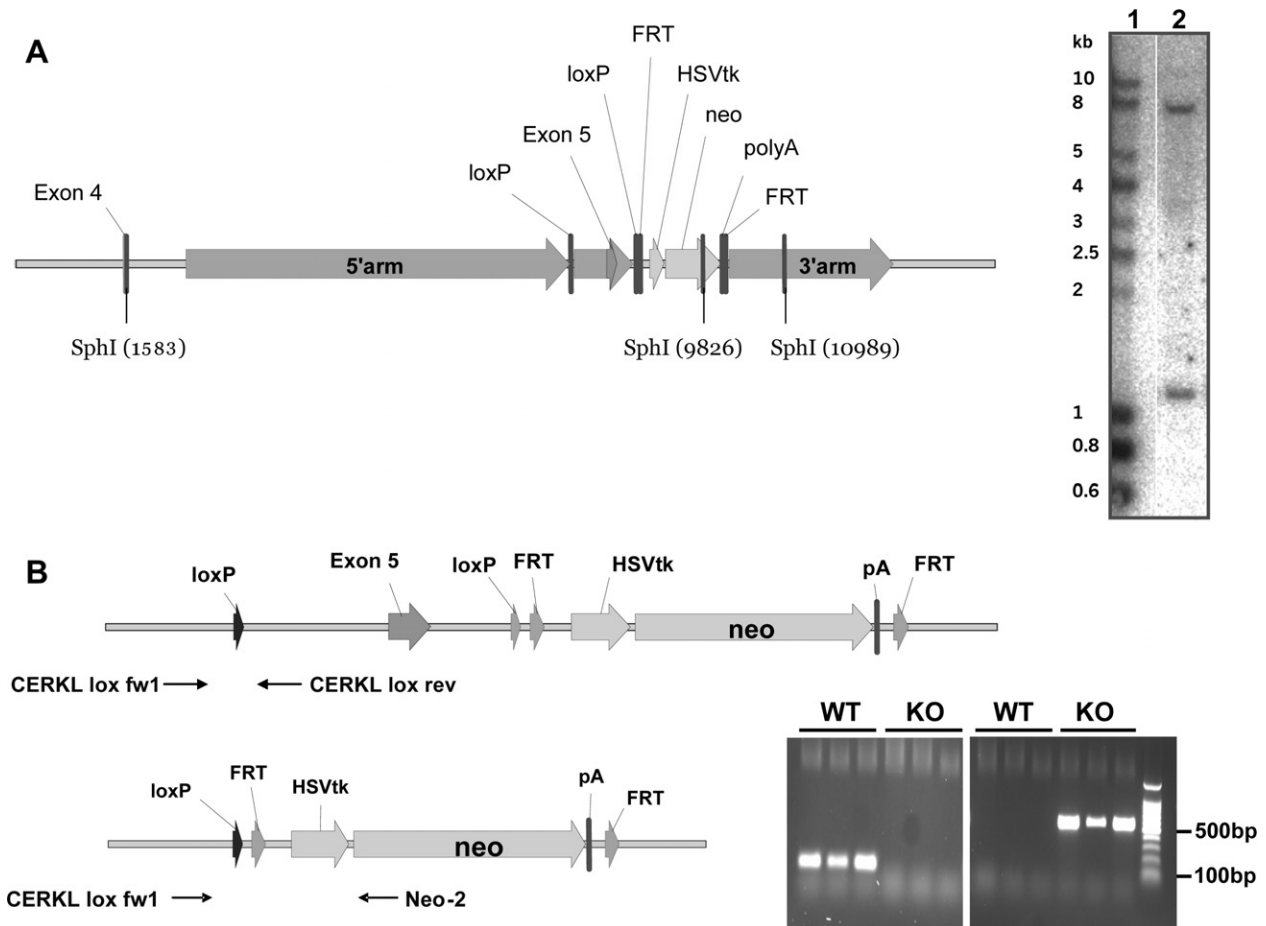


**Fig. 1.** Disruption of the *CerKL* gene in the mouse genome. (A) Left: schema showing the targeting cassette after homologous recombination of pCERKL target into the endogenous *CerKL* locus and the location of the SphI restriction sites. Right: Southern blot after SphI digestion of DNA from mouse ES cell clones. 1: DNA marker; 2: example of a positive clone. (B) Left: schema showing the targeted *CerKL* locus before and after Cre/loxP recombination. The *CerKL* locus before Cre/loxP recombination contains exon 5, whereas exon 5 is excised from the locus after Cre-mediated excision. Right: PCR to detect the *CerKL* KO allele. With primers fw and rw a 133-bp fragment is amplified from the WT allele but not from the KO allele, whereas with primers fw and neo a 550-bp fragment is amplified from the KO allele only.

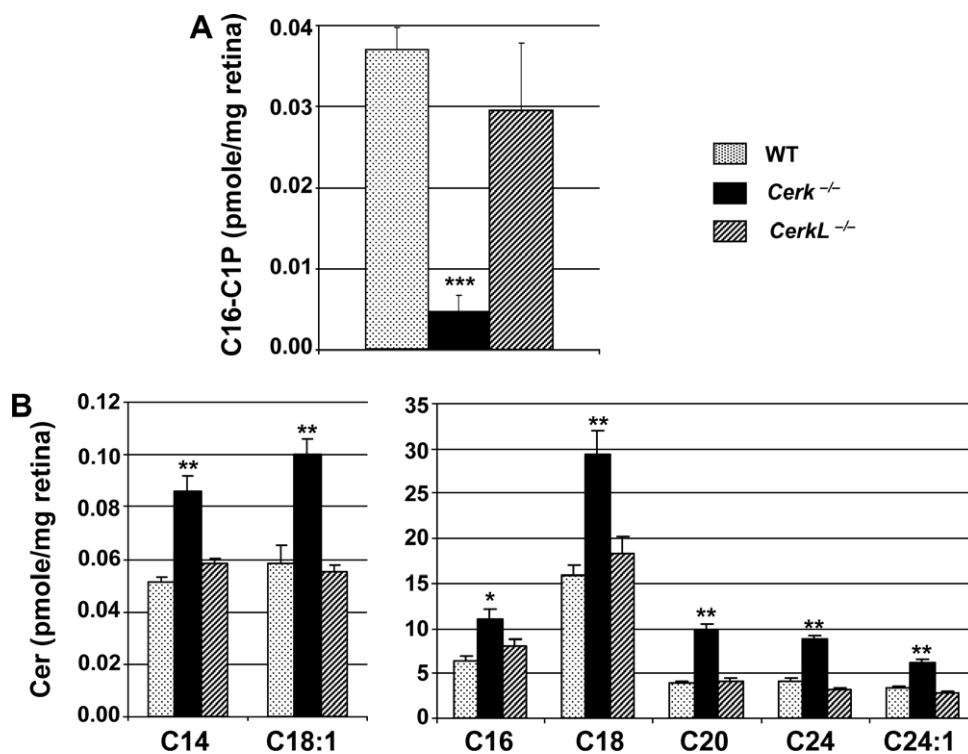


**Fig. 2.** Cer and C16-C1P levels are not modified in *CerKL*<sup>-/-</sup> retinas. Retinal Cer and C1P levels were measured in isolated retinas after lipid extraction followed by LC/MS analysis as described in the Experimental procedures section. We used 12 animals per strain and, for each animal, one retina was used for C1P analysis and the other for Cer analysis. Measurements were performed on triplicates of four retinas each. Statistical significance was evaluated with a Student *t* test (\**p* < 0.05; \*\**p* < 0.01; \*\*\**p* < 0.001). (A) Concentration of C16-C1P in the retina of WT (dotted bar), *CerK*<sup>-/-</sup> (black bar), and *CerKL*<sup>-/-</sup> (hatched bar) animals. (B) Concentrations of C14-Cer, C16-Cer, C18-Cer, C18:1-Cer, C20-Cer, C24-Cer, and C24:1-Cer in the retina of WT (dotted bar), *CerK*<sup>-/-</sup> (black bar), and *CerKL*<sup>-/-</sup> (hatched bar) animals.

#### Phosphorylation of endogenous Cer in the retina of *CerKL*<sup>-/-</sup> mice

To further check if *CerKL* might be able to act as a bona fide Cer kinase, we labeled isolated retinas with <sup>33</sup>P orthophosphate and analyzed Cer phosphorylation by measuring newly formed endogenous C1P. Labeled C1P was readily detected in WT retinas (Fig.

3A). Remarkably, no C1P could be detected in *CerK*<sup>-/-</sup> retinas (Fig. 3B). In *CerKL*<sup>-/-</sup> retinas, however, C1P was detected to a level similar to that found in WT retinas (Fig. 3C). These results demonstrate that the Cer kinase activity detected in whole retina *ex vivo* may be entirely attributed to *CerK*; *CerKL* does not appear to contribute to retinal Cer phosphorylation.

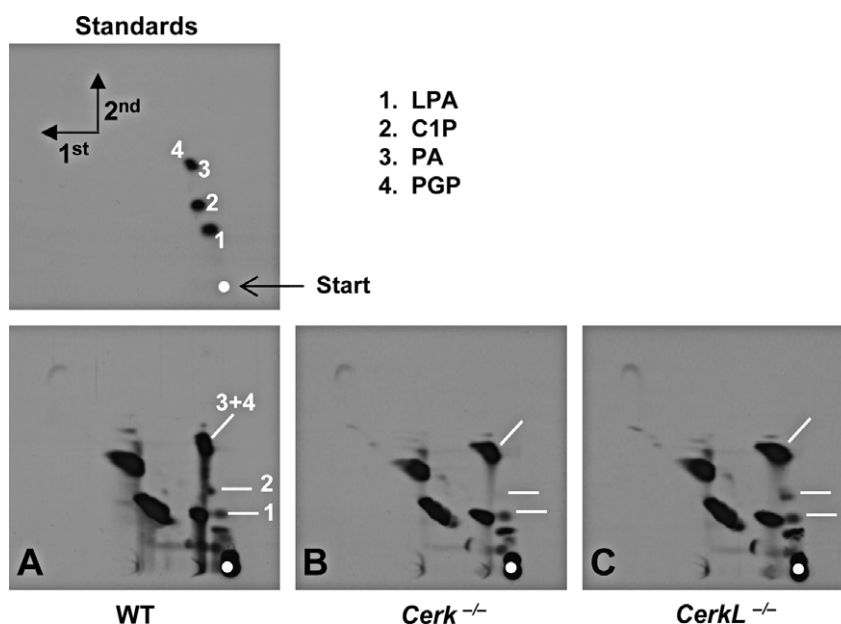


**Fig. 3.** *De novo* phosphorylation of Cer into C1P occurs in *CerKL*<sup>-/-</sup> retinas. Whole retinas from WT (A), *CerK*<sup>-/-</sup> (B) or *CerKL*<sup>-/-</sup> (C) animals were labeled in <sup>33</sup>P orthophosphate-containing DMEM for 2 h. Lipids were then harvested and run using 2-dimensional TLC. LPA, C1P, PA, and PGP were prepared separately, as described in the Experimental procedures section, subsequently pooled and run under conditions identical to those used for retinal lipid extracts.



To further investigate which lipid substrate might be recognized by CerKL, we labeled LPA, PA, and PGP and used them as standards. These lipid products can be produced by related enzymes of the DAGK family to which CerKL belongs [12–14]. There was no difference in the levels of the labeled phospholipids corresponding to these standards in *CerKL*<sup>−/−</sup> compared with WT retinas. Prior work from our lab also showed that sphingosine cannot be phosphorylated by CerKL [7]. Altogether, these results indicate that the currently reported substrates used by DAGK family members may not serve as substrates for CerKL.

In conclusion, this work shows that CerKL does not contribute to phosphorylation of Cer and has no impact on Cer and C16-C1P levels in the retina. This is in contrast to CerK, which therefore appears to be a major if not the unique retinal Cer kinase. Furthermore, CerKL is unlikely to contribute to phosphorylation of known lipid substrates for related kinases. CerKL, therefore, stands as an orphan kinase; characterization of its activity remains a key challenge to understanding why its deficiency leads to retinitis pigmentosa.

### Acknowledgments

We are grateful to Roland Reuschel and Waltraud Mayer-Granitzer for help with ceramide measurements, to Werner Hoellriegel and his team for animal care taking, to Susanna Huber for PCR genotyping, to Julie Boisclair and her laboratory for histopathological analyses, and to Elizabeth Morgan for editorial work on this manuscript.

### References

- [1] D.T. Hartong, E.L. Berson, T.P. Dryja, Retinitis pigmentosa, *Lancet* 368 (2006) 1795–1809.
- [2] M. Tuson, G. Marfany, R. Gonzalez-Duarte, Mutation of CERKL, a novel human ceramide kinase gene, causes autosomal recessive retinitis pigmentosa (RP26), *Am. J. Hum. Genet.* 74 (2004) 128–138.
- [3] M. Sugiura, K. Kono, H. Liu, T. Shimizugawa, H. Minekura, S. Spiegel, T. Kohama, Ceramide kinase, a novel lipid kinase. Molecular cloning and functional characterization, *J. Biol. Chem.* 277 (2002) 23294–23300.
- [4] A. Gomez-Munoz, Ceramide 1-phosphate/ceramide, a switch between life and death, *Biochim. Biophys. Acta* 1758 (2006) 2049–2056.
- [5] C. Graf, P. Rovina, L. Tauzin, A. Schanzer, F. Bornancin, Enhanced ceramide-induced apoptosis in ceramide kinase overexpressing cells, *Biochem. Biophys. Res. Commun.* 354 (2007) 309–314.
- [6] P. Mitra, M. Maceyka, S.G. Payne, N. Lamour, S. Milstien, C.E. Chalfant, S. Spiegel, Ceramide kinase regulates growth and survival of A549 human lung adenocarcinoma cells, *FEBS Lett.* 581 (2007) 735–740.
- [7] F. Bornancin, D. Mechtcheriakova, S. Stora, C. Graf, A. Wlachs, P. Devay, N. Urtz, T. Baumruker, A. Billich, Characterization of a ceramide kinase-like protein, *Biochim. Biophys. Acta* 1687 (2005) 31–43.
- [8] Y. Inagaki, S. Mitsutake, Y. Igarashi, Identification of a nuclear localization signal in the retinitis pigmentosa-mutated RP26 protein, ceramide kinase-like protein, *Biochem. Biophys. Res. Commun.* 343 (2006) 982–987.
- [9] F. Schwenk, U. Baron, K. Rajewsky, A cre-transgenic mouse strain for the ubiquitous deletion of loxP-flanked gene segments including deletion in germ cells, *Nucleic Acids Res.* 23 (1995) 5080–5081.
- [10] C. Graf, B. Zemmann, P. Rovina, N. Urtz, A. Schanzer, R. Reuschel, D. Mechtcheriakova, M. Müller, E. Fischer, C. Reichel, S. Huber, J. Dawson, J.G. Meingassner, A. Billich, S. Niwa, R. Badegruber, P.P. Van Veldhoven, B. Kinzel, T. Baumruker, F. Bornancin, Neutropenia with impaired immune response to *Streptococcus pneumoniae* in ceramide kinase-deficient mice, *J. Immunol.* 180 (2008) 3457–3466.
- [11] A. Boath, C. Graf, E. Lidome, T. Ullrich, P. Nussbaumer, F. Bornancin, Regulation and traffic of ceramide-1-phosphate produced by ceramide kinase: comparative analysis of glucosylceramide and sphingomyelin, *J. Biol. Chem.* 283 (2008) 8517–8526.
- [12] S. Spiegel, S. Milstien, Functions of the multifaceted family of sphingosine kinases and some close relatives, *J. Biol. Chem.* 282 (2007) 2125–2129.
- [13] F. Sakane, S. Imai, M. Kai, S. Yasuda, H. Kanoh, Diacylglycerol kinases: why so many of them?, *Biochim. Biophys. Acta* 1771 (2007) 793–806.
- [14] H.M.A. Bakali, M.D. Herman, K.A. Johnson, A.A. Kelly, A. Wieslander, B.M. Hallberg, P. Nordlund, Crystal structure of YegS, a homologue to the mammalian diacylglycerol kinases, reveals a novel regulatory metal binding site, *J. Biol. Chem.* 282 (2007) 19644–19652.